Current Medical Science
DOI https://doi.org/10.1007/s11596-023-2731-8
43(3):560-571,2023

ARID1A Inactivation Increases Expression of circ0008399 and Promotes Cisplatin Resistance in Bladder Cancer*

Yang-kai JIANG[1†], Yu-jun SHUAI[1†], Hua-min DING[2†], Hui ZHANG[1], Chao HUANG[1], Liang WANG[1], Jia-yin SUN[1], Wen-jie WEI[1], Xing-yuan XIAO[1#], Guo-song JIANG[1#]

[1]*Department of Urology, Union Hospital, Tongji Medical College, Huazhong University of Science and Technology, Wuhan 430022, China*

[2]*Department of Urology, Jingshan Union Hospital of Huazhong University of Science and Technology (People's Hospital of Jingshan), Jingshan 431899, China*

[Abstract] Objective: Cisplatin (CDDP)-based chemotherapy is a first-line, drug regimen for muscle-invasive bladder cancer (BC) and metastatic bladder cancer. Clinically, resistance to CDDP restricts the clinical benefit of some bladder cancer patients. AT-rich interaction domain 1A (ARID1A) gene mutation occurs frequently in bladder cancer; however, the role of CDDP sensitivity in BC has not been studied. **Methods:** We established ARID1A knockout BC cell lines using CRISPR/Cas9 technology. IC_{50} determination, flow cytometry analysis of apoptosis, and tumor xenograft assays were performed to verify changes in the CDDP sensitivity of BC cells losing ARID1A. qRT-PCR, Western blotting, RNA interference, bioinformatic analysis, and ChIP-qPCR analysis were performed to further explore the potential mechanism of ARID1A inactivation in CDDP sensitivity in BC. **Results:** It was found that ARID1A inactivation was associated with CDDP resistance in BC cells. Mechanically, loss of ARID1A promoted the expression of eukaryotic translation initiation factor 4A3 (EIF4A3) through epigenetic regulation. Increased expression of EIF4A3 promoted the expression of hsa_circ_0008399 (circ0008399), a novel circular RNA (circRNA) identified in our previous study, which, to some extent, showed that ARID1A deletion caused CDDP resistance through the inhibitory effect of circ0008399 on the apoptosis of BC cells. Importantly, EIF4A3-IN-2 specifically inhibited the activity of EIF4A3 to reduce circ0008399 production and restored the sensitivity of ARID1A inactivated BC cells to CDDP. **Conclusion:** Our research deepens the understanding of the mechanisms of CDDP resistance in BC and elucidates a potential strategy to improve the efficacy of CDDP in BC patients with ARID1A deletion through combination therapy targeting EIF4A3.

Key words: AT-rich interaction domain 1A; hsa_circ_0008399; eukaryotic translation initiation factor 4A3; cisplatin resistance; bladder cancer

Bladder cancer (BC) is the 10th most common cancer and 14th most frequent cause of cancer death worldwide[1]. It is classified into non-muscle-invasive BC (NMIBC) and muscle-invasive BC (MIBC)[2]. MIBC accounts for approximately 25% of initially diagnosed BC cases, and up to 10% to 20% of patients with NMIBC will progress to MIBC[3, 4]. Worse still, approximately 5% to 15% of BC patients present with metastatic disease at the time of initial diagnosis[5]. Currently, cisplation (CDDP)-based combination chemotherapy is identified as the mainstay of treatment for advanced, metastatic BC[6]. Although cisplatin therapy has a certain initial response rate, it is prone to failure due to the development of chemotherapeutic resistance[7]. Therefore, it is important to study the underlying mechanism of CDDP resistance and improve the sensitivity of BC patients to CDDP chemotherapy.

The AT-rich interaction domain 1A (ARID1A)

Yang-kai JIANG, E-mail: 2093079839@qq.com; Yu-jun SHUAI, E-mail: shuaiyujun20@163.com; Hua-min DING, E-mail: 873806112@qq.com

†These authors contributed equally to this work.

#Corresponding authors, Guo-song JIANG, E-mail: jiangguosongdoc@hotmail.com; Xing-yuan XIAO, E-mail: xiaoxy@hust.edu.cn

*This work was supported by grants from the National Natural Science Foundation of China (No. 81974396, No. 81874091, No. 82072840, and No. 82102734), the Natural Science Foundation of Hubei Province (No. 2020CFB829), and the Health Commission of Hubei Province Scientific Research Project (No. WJ2021F081).

Electronic supplementary material The online version of this article (https://doi.org/10.1007/s11596-023-2731-8) contains supplementary material, which is available to authorized users.

gene encodes a core member of the switching/sucrose non-fermentable family (SWI/SNF) complex[8], whose members have helicase and ATPase activities and are thought to regulate transcription of certain genes by altering the chromatin structure around those genes[9]. ARID1A is the most frequently mutated subunit in the SWI/SNF complex across all human cancers[10, 11]. Mutations and loss of the ARID1A gene mostly lead to its inactivation and ARID1A protein loss[12]. ARID1A inactivation affects the biological functions of multiple tumor cells, such as proliferation, metastasis, differentiation, and apoptosis[13–17]. ARID1A gene silencing reduces the sensitivity of ovarian clear cell carcinoma to cisplatin through activating the PI3K-AKT signaling pathway[18]. However, the association between ARID1A inactivation and BC chemotherapy sensitivity has not yet been explored.

Circular RNAs (circRNAs) are closed RNA transcripts produced by back-splicing of a single pre-mRNA[19]. With the development of next generation sequencing and bioinformatics technology, a growing number of circRNAs have been identified, characterized, and functionally annotated. It was found that the distribution and effects of circRNAs were systematically altered in cancers, demonstrating their important influence on the occurrence and development of cancers[20]. Our previous studies found that circHIPK3, BCRC-3, circNR3C1, has_circ_0001361, and circLIFR could play critical roles in cell proliferation, metastasis, invasion, and chemotherapy sensitivity during BC progression[21–25]. In a recent study, we discovered that circ0008399, generated from the circularization of exons 2, 3, 4, 5, and 6 in the RBM3 gene, was upregulated by eukaryotic translation initiation factor 4A3 (EIF4A3) in BC. Functionally, high expression of circ0008399 could inhibit cell apoptosis and reduce the chemotherapy sensitivity of BC to CDDP *in vitro* and *in vivo*. Mechanistically, circ0008399 could interact with WTAP to promote the formation of m6A methyltransferase complex, which promotes the expression of TNFAIP3 by increasing its mRNA stability in an m6A-dependent manner, thereby reducing the activity of caspase 8. In conclusion, our previous studies have preliminarily explained the novel mechanism of circ0008399/WTAP-mediated m6A-dependent regulation of TNFAIP3 and highlighted the role of circ0008399 in regulating chemotherapy sensitivity of CDDP in BC[26]. Nonetheless, the role of circRNAs in CDDP sensitivity of BC with ARID1A deletion remains to be further elucidated.

In this study, we constructed ARID1A knockout BC cell lines using CRISPR/Cas9 technology and verified that the loss of ARID1A could reduce the sensitivity of BC cells to CDDP *in vitro* and *in vivo*. Mechanistically, we found that the loss of ARID1A reduced histone deacetylase 1 (HDAC1) recruitment to chromatin, promoted bromodomain containing 4 (BRD4)-mediated activation of EIF4A3 transcription, and subsequently increased the expression of circ0008399. Importantly, we found that inhibition of EIF4A3 expression by EIF4A3-IN-2, a small molecule inhibitor of EIF4A3, could reduce circ0008399 production and enhance the chemotherapy sensitivity of BC cells with ARID1A inactivation to CDDP. Taken together, these findings highlight an effective combination therapy of EIF4A3-IN-2 and CDDP to fight against cisplatin resistance caused by the mutation of ARID1A, thereby improving the clinical prognosis of related patients.

1 MATERIALS AND METHODS

1.1 Cell Culture and Treatment

The human BC cell line EJ was obtained from The American Type Culture Collection (ATCC, USA). The human metastatic BC cell line, T24T, which is a lineage-related lung metastatic variant of the invasive bladder cancer cell line T24, was provided by Dr. Dan Theodorescu (Department of Urology, University of Virginia, USA). All the cell lines were cultured in RPMI-1640 medium (Gibco, USA) supplemented with 10% fetal bovine serum (FBS, Gibco, Australia) and 1% penicillin/streptomycin (Gibco, USA) in the recommended media at 37°C supplied with 5% CO_2. Cells were authenticated by short tandem repeat profiling and tested negative for mycoplasma contamination.

Cisplatin (Sigma, USA) was solubilized in DMSO. EIF4A3-IN-2 (HY-101785, MCE, USA), a highly selective and noncompetitive eukaryotic initiation factor 4A-3 (EIF4A3) inhibitor with half maximal inhibitory concentration (IC_{50}) of 110 nmol/L[27, 28], was solubilized in DMSO. (+)-JQ-1 (JQ1, HY-13030, MCE, USA), a specific and reversible BET bromodomain inhibitor[29], was solubilized in DMSO.

1.2 CRISPR/Cas9 Knockout

EJ and T24T cells were transfected with the pSpCas9(BB)-2A-Puro (PX459) plasmid (Addgene, USA) containing ARID1A single-guide RNAs (sgRNAs) by using Lipofectamine 2000 (Invitrogen, USA), following the manufacturer's instructions. The sgRNAs for the ARID1A gene were designed using the web tool CHOPCHOP (http://chopchop.cbu.uib.no) and were synthesized by TSINGKE (China) (table 1). As a control, we used pSpCas9(BB)-2A-Puro (PX459) plasmid that did not undergo CRISPR-Cas9-mediated gene editing. Cells were selected in the presence of 1 μg/mL puromycin (Invitrogen, USA) for 2 weeks, followed by seeding into a 96-well plate to isolate individual colonies. Deletion was verified by Western blotting with the anti-ARID1A antibody (Cat. No.

Table 1 The sequences of primers and oligonucleotides used in this study

Primers and oligonucleotides	Sequence (5′–3′)
Primers for PCR	
Divergent-circ0008399 F	GGCTATGGGAGTGGCAGGTATT
Divergent-circ0008399 R	TCGTCGGTGTTAAAGTTGAGCC
Divergent-circLIFR F	ACGTAAAGAGAGTATGGAGCTCGT
Divergent-circLIFR R	TGTTCCAGAGGGTGCTTTCCA
GAPDH F	TGCAACCGGGAAGGAAATGAA
GAPDH R	CGCCCAATACGACCAAATCAG
EIF4A3 F	CCGCATCTTGGTGAAACGTGAT
EIF4A3 R	GCCTGAGTGATGGTCAGTGTGT
EIF4A3 F (ChIP)	AGATAGCCCCGCCTCGAATA
EIF4A3 R (ChIP)	CCGTGAGGGTTTCCACTCG
sgRNAs	
ARID1A sgRNA#1F	CAACGAAGAACTCGAACGGGAACGC
ARID1A sgRNA#1R	AAACGCGTTCCCGTTCGAGTTCTTC
ARID1A sgRNA#2F	CAACGCAGCAGAACTCTCACGACCA
ARID1A sgRNA#2R	AAACTGGTCGTGAGAGTTCTGCTGC
ARID1A sgRNA#3F	CAACGCTTCGGGCAACCCTACGGC
ARID1A sgRNA#3R	AAACGCCGTAGGGTTGCCCGAAGC
siRNAs	
si-circ0008399#1	GCACATAATATAGGACTTGAA
si-circ0008399#2	ATATAGGACTTGAACTGCCAT
si-NC (scramble)	GAACCAGAGGAGGTGGCTTTGG

ARID1A: AT-rich interaction domain 1A; ChIP: chromatin immunoprecipitation; circ0008399: circular RNA 0008399; circLIFR: circular RNA LIFR; EIF4A3: eukaryotic initiation factor 4A3; F: forward primer; GAPDH: glyceraldehyde-3-phosphate dehydrogenase; NC: negative control; PCR: polymerase chain reaction; R: reverse primer; sgRNA: single guide RNA; siRNA: small interfering RNA

A19570; 1:1000; Abclonal, China).

1.3 Western Blotting

Cellular proteins were extracted with RIPA lysis buffer (Thermo Scientific, USA) according to the instructions. A Western blotting assay was performed as previously described[25]. Briefly, the protein samples were subjected to SDS-PAGE and then transferred to a PVDF membrane, followed by a block with 5% non-fat milk. Membranes were efficiently incubated with primary antibodies overnight at 4°C on a shaker, and incubated with HRP-conjugated secondary antibodies for 1 h at room temperature before visualizing bands via a Bio Spectrum 600 Imaging System (UVP, USA). The following antibodies were used: primary antibodies against ARID1A (Cat. No. A19570; 1:1000; Abclonal, China), EIF4A3 (Cat. No. A8985; 1:1000; Abclonal, China), HDAC1 (Cat. No.10197-1-AP; 1:10000; Proteintech, USA), Histone H4 acetylation (H4Ac) (pan-acetyl; Cat. No.39244; 1:5000; Proteintech, USA), bromodomain containing 4 (BRD4) (Cat. No.67374-2-Ig; 1:4000; Proteintech, USA) and GAPDH (Cat. No. 60004-1-Ig; 1:5000; Proteintech, USA); HRP-conjugated secondary goat anti-rabbit antibody (Cat. No. SA00001-2; 1:4000; Proteintech, USA).

1.4 IC_{50} Determination

The ARID1A-WT and ARID1A-KO cells were seeded into a 96-well plate at a density of 10 000 cells per well and were cultured in a cell culture chamber overnight. Then, the cells were treated with a series of dilute concentrations of cisplatin (0, 1, 2, 4, 6, 8, 10, 12, 14, 16, 18, and 20 μmol/L; Sigma, USA) for 24 h. Cell viability was measured by the Cell Counting Kit-8 (CCK-8) assay (Dojindo, Japan) according to the manufacturer's instructions. The dose-response curve at different concentrations was charted to calculate the IC_{50} using a Probit regression model. Each concentration included 5 replicating wells, and the experiments were performed 3 times independently to obtain a mean value of IC_{50}[30].

1.5 Apoptosis Assay

The cell apoptosis assay was performed according to the manual of the Annexin V-FITC/PI apoptosis detection kit (Vazyme, China) with some modifications. Briefly, BC cells were seeded into a 6-well plate administered with CDDP or DMSO. They were collected and resuspended in 100 μL 1× binding buffer and then incubated with 5 μL Annexin V-FITC and 5 μL PI Staining Solution in the dark at room temperature for 10–15 min. Subsequently, the samples were analyzed by flow cytometry (Becton Dickinson, USA). Normal live cells were Annexin V-FITC negative and PI negative; early apoptotic cells were Annexin V-FITC positive and PI negative; and late apoptotic or necrotic cells were Annexin V-FITC positive and PI positive. All data were analyzed using FlowJo software (FlowJo_V10).

1.6 Reverse Transcriptase Polymerase Chain Reaction and Quantitative Real-time Polymerase Chain Reaction

Total RNA was isolated from cells with a RNeasy mini kit (QIAGEN, Germany) according to the manufacturer's instructions. cDNA was synthesized using HiScript Ⅲ RT SuperMix (Vazyme, China). The quantitative real-time polymerase chain reaction (qRT-PCR) analyses were performed using SYBR green master mix (Vazyme, China) and primers (table 1). Then the test was carried out with the StepOnePlus Real-Time PCR System (Applied Biosystems, USA), and the results of RNA levels were analyzed using the $2^{-\Delta\Delta Ct}$ method.

1.7 RNA Interference and Cell Transfection

The siRNAs were synthesized by RiboBio (China), targeting circ0008399 splice sites (table 1). The cells were seeded into a 6-well plate cultured in cell culture chamber overnight. SiRNAs at a final concentration of 50 nmol/L were transfected into cells using RNAiMAX (Invitrogen, USA) according to the manufacturer's instructions. The RNA interference silencing efficiency was measured by qRT-PCR 24 h after transfection.

1.8 Chromatin Immunoprecipitation and Chromatin Immunoprecipitation Quantitative Polymerase Chain Reaction Assay

Chromatin immunoprecipitation (CHIP) assays were performed using a ChIP assay kit (Beyotime, China) with some modifications. Briefly, the cells were fixed with 1% formaldehyde at final concentration to cross-link the target protein with the corresponding genomic DNA. Then, the cells were lysed and sonicated (Sonics Vibra-Cell™, USA; a 20 s pulse and 30 s off at 25% amplitude and 3 min) to shear the genomic DNA into 200–1000 bp sizes. Next, sonicated lysates were incubated with ChIP antibodies against HDAC1 (Cat. No. 10197-1-AP; Proteintech, USA), H4Ac (pan-acetyl; Cat. No. 39244; Proteintech, USA) and BRD4 (Cat. No. 91302; Proteintech, USA) or IgG control (Cat. No. 30000-0-AP; Proteintech, USA). The precipitates obtained were used for Western blotting, or DNA was isolated for qPCR of the target gene sequence. The relative ChIP enrichments were confirmed by ChIP-qPCR and compared with an IgG control as fold enrichment. ChIP-qPCR primers for the EIF4A3 promoter are listed in table 1.

1.9 Bioinformatic Analysis

The ChIP sequencing (ChIP-seq) data (Cistrome-DB ID: 58462,8657,43092,91532) were obtained from Cistrome Data Browser (CistromeDB, http://cistrome.org/db) and the ChIP-seq peaks were visualized using the UCSC genome browser (http://genome.ucsc.edu).

1.10 Tumor Xenografts Assay

The 4-week-old female BALB/C nude mice were purchased from the Beijing Vital River Lab Animal Technology Co., Ltd. The mice were randomly divided into 4 groups (n=6 each), and 2×10^6 ARID1A-WT or ARID1A-KO T24T cells were injected subcutaneously into the right dorsal side of the mice. At 3rd day after injection, CDDP or PBS was administered by intraperitoneal injection twice a week at the dose of 2 mg/kg. The volumes of the tumors were measured with a caliper every 3 days with following formula: V=Length × $Width^2$ ×0.5. After 35 days, the mice were sacrificed and examined for tumor weight. All animal experiments were carried out in accordance with NIH guidelines for the care and use of laboratory animals and were approved by the Animal Care Committee of Tongji Medical College (IACUC number: 2021–2589).

1.11 Statistical Analysis

All the data statistical analyses were performed using GraphPad Prism 9.2.0 software (La Jolla, USA). A student's t test and ANOVA were applied to assess the statistical significance between groups. Data are presented as mean ± s the standard deviation (SD). P<0.05 was considered to be statistically significant.

2 RESULTS

2.1 Knockout of ARID1A Decreases Sensitivity of BC to CCDP *In Vitro*

To elucidate the effect of ARID1A inactivating mutation on the sensitivity of BC to CDDP chemotherapy, we used CRISPR/Cas9 gene-editing technology to establish ARID1A-knockout (KO) EJ and T24T cell lines. The KO efficacy was verified by Western blotting (fig. 1A and 1B). The IC_{50} value of CDDP was increased when ARID1A was knocked out in BC cells (fig. 1C and 1D). Consistently, the ARID1A KO significantly decreased the CDDP-induced apoptosis in BC cells, while ARID1A KO had little effect on apoptosis of BC cells without CDDP treatment compared with wild-type BC cells (fig. 1E–1H). These results suggested that the ARID1A KO was functionally associated with chemotherapy sensitivity in BC.

2.2 Knockout of ARID1A Decreases Sensitivity of BC to CCDP *In Vivo*

To further explore the *in vivo* evidence for the above results, we observed the sensitivity of BC cells with KO of ARID1A to CDDP *in vivo*. T24T cells of wild-type (ARID1A-WT) or ARID1A-KO were injected subcutaneously into BALB/c nude mice and allowed to grow for 3 days to establish subcutaneous xenograft tumor. Then, the mice were randomly assigned into 4 groups and administered with the dose of 2 mg/kg CDDP or PBS twice a week. The tumor growth was monitored continuously up to 35 days (fig. 2A). The ARID1A KO slightly but consistently influenced the tumor volume and weight of subcutaneous xenografts, while it could significantly attenuate the CDDP-induced

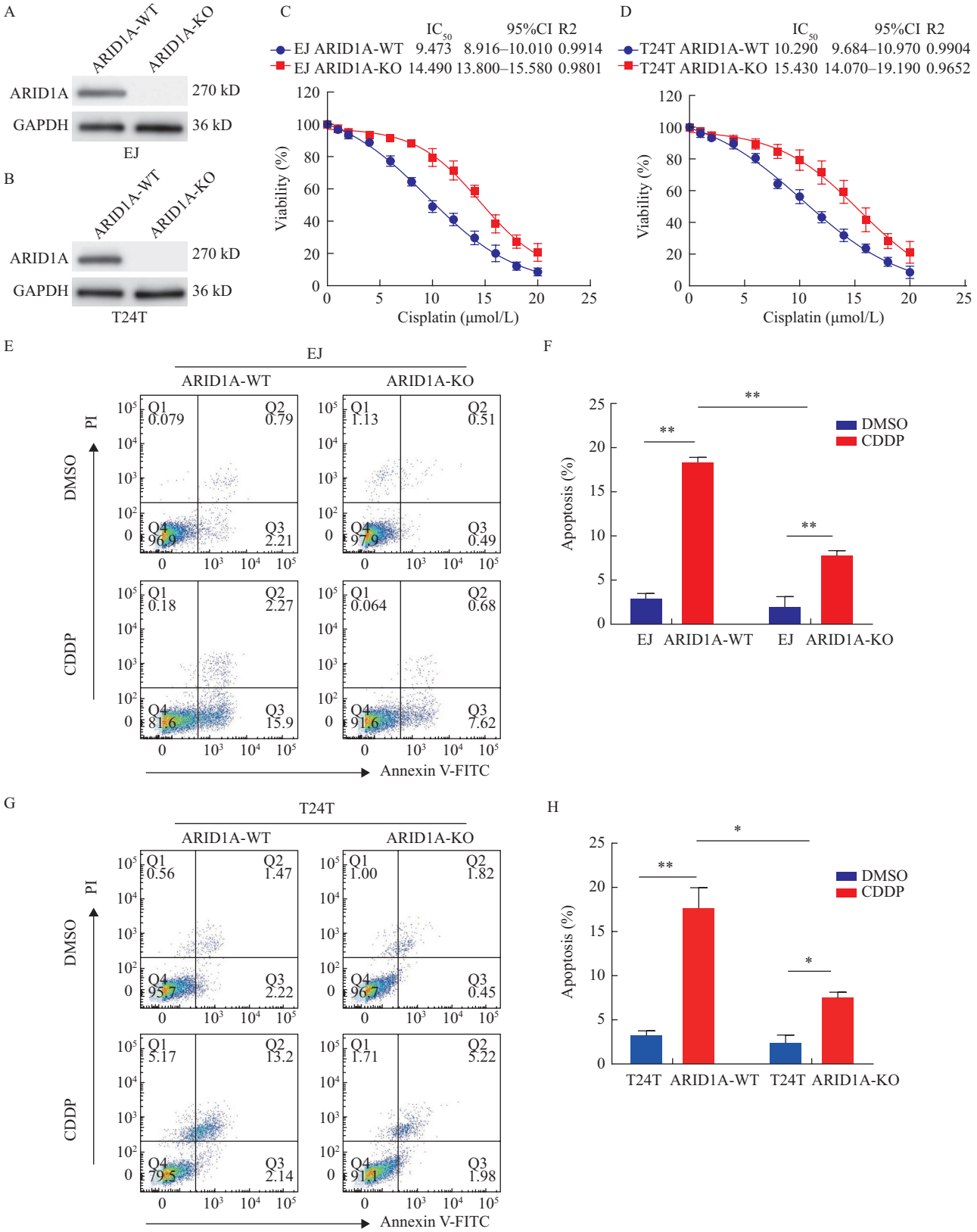

Fig. 1 Knockout of ARID1A decreases the sensitivity of BC to CDDP *in vitro*

A and B: Western blotting analysis showed ARID1A protein levels in EJ and T24T cells of ARID1A-WT and ARID1A-KO. Protein levels were normalized by GAPDH. C: the determination of IC_{50} values after treatment with CDDP for 24 h in ARID1A-WT and ARID1A-KO EJ cells. D: the determination of IC_{50} values after treatment with CDDP for 24 h in ARID1A-WT and ARID1A-KO T24T cells. E and F: Flow cytometry revealed the CDDP-induced apoptosis rate in EJ cells treated with 5 μmol/L CDDP for 24 h. G and H: Flow cytometry revealed the CDDP-induced apoptosis rate in T24T cells treated with 5 μmol/L CDDP for 24 h. The data were reported as the mean ± SD (n=3) of the individual experiments. Statistical significance by two-way ANOVA in F and H: $^{*}P<0.05$, $^{**}P<0.01$. ARID1A: AT-rich interaction domain 1A; BC: bladder cancer; CDDP: cisplatin; GAPDH: glyceraldehyde-3-phosphate dehydrogenase; IC_{50}: half maximal inhibitory concentration; KO: knockout; SD: standard deviation; WT: wild-type

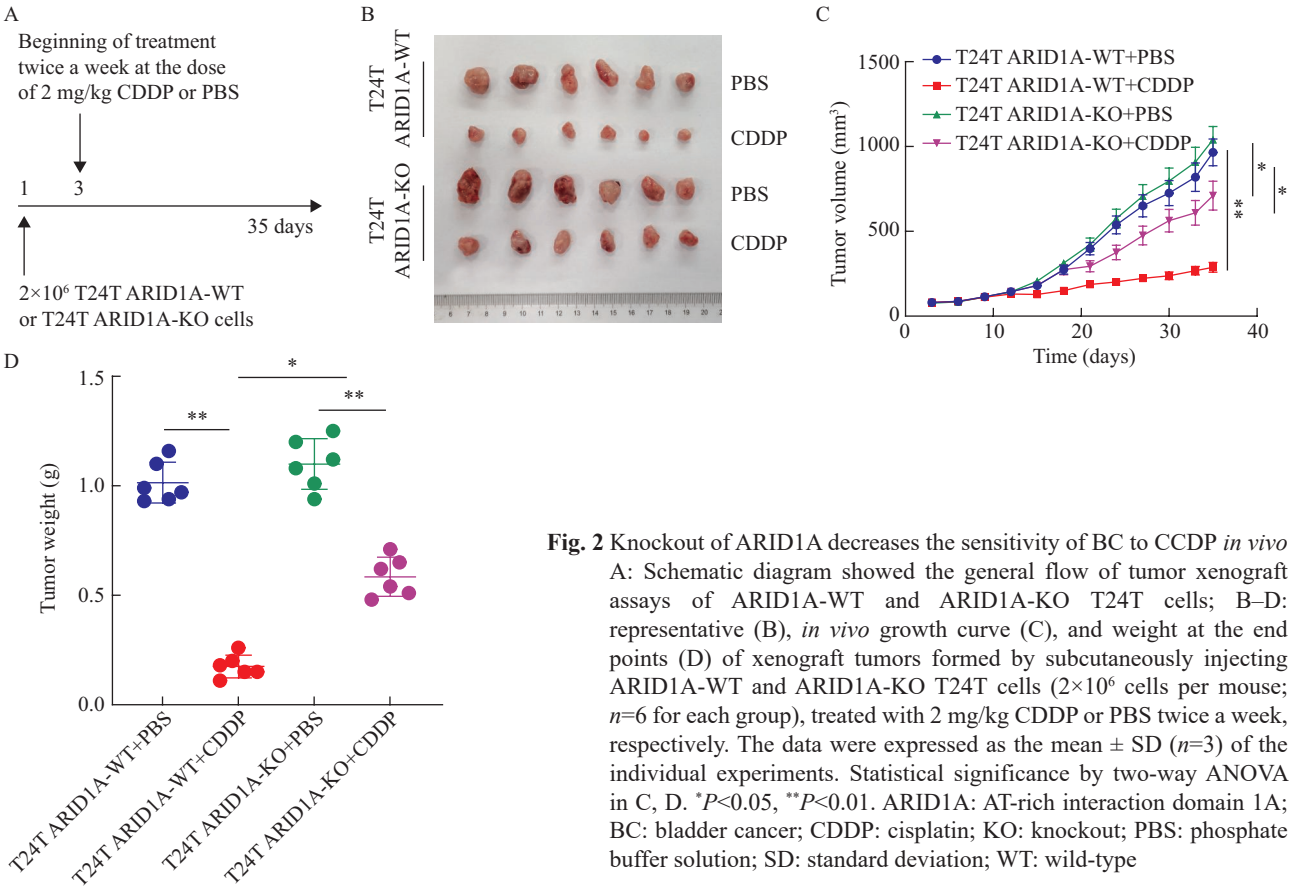

Fig. 2 Knockout of ARID1A decreases the sensitivity of BC to CCDP *in vivo*
A: Schematic diagram showed the general flow of tumor xenograft assays of ARID1A-WT and ARID1A-KO T24T cells; B–D: representative (B), *in vivo* growth curve (C), and weight at the end points (D) of xenograft tumors formed by subcutaneously injecting ARID1A-WT and ARID1A-KO T24T cells (2×10^6 cells per mouse; n=6 for each group), treated with 2 mg/kg CDDP or PBS twice a week, respectively. The data were expressed as the mean ± SD (n=3) of the individual experiments. Statistical significance by two-way ANOVA in C, D. $^*P<0.05$, $^{**}P<0.01$. ARID1A: AT-rich interaction domain 1A; BC: bladder cancer; CDDP: cisplatin; KO: knockout; PBS: phosphate buffer solution; SD: standard deviation; WT: wild-type

inhibition in growth of subcutaneous xenograft tumors (fig. 2B–2D). Collectively, our findings demonstrated that loss of ARID1A increased resistance to CDDP in BC *in vivo*.

2.3 Loss of ARID1A Induces Expression of circ0008399

Our previous studies have discovered 2 new circRNAs, circLIFR and circ0008399, which are related to the sensitivity of CDDP chemotherapy in BC[25, 26]. To further explore whether these circRNAs have a potential function in CDDP resistance in ARID1A-null BC, we attempted to detect the expression level of circLIFR and circ0008399 in ARID1A-WT and ARID1A-KO cells by qRT-PCR. We found that the expression level of circ0008399 was significantly elevated when ARID1A was lost, whereas the expression of circLIFR did not change significantly (fig. 3A). These results suggested that the increased expression of circ0008399 might be involved in the inactivation of ARID1A-mediated reduced sensitivity to CDDP chemotherapy in BC.

To further confirm the function of circ0008399 on CDDP chemotherapy sensitivity in ARID1A inactivated BC cells, we performed a rescue experiment by knocking down circ0008399 in ARID1A KO BC cells. The interference effects of siRNAs targeting circ0008399 were verified by qRT-PCR (fig. 3B), and si-circ0008399#1 was selected for subsequent experiments because of its higher interference efficiency. Importantly, we confirmed that KO of circ0008399 significantly restored the ARID1A KO-mediated decrease of CDDP sensitivity in EJ and T24T cells (fig. 3C–3F). Hence, these results suggested that the loss of ARID1A induced the expression of circ0008399, and inhibition of circ0008399 expression resulted in increased CDDP chemosensitivity in ARID1A-deficient BC.

2.4 Inhibition of EIF4A3 Promotes Chemosensitivity of ARID1A-deficient Bladder Cancer Cells to CDDP

Our previous results showed that EIF4A3 could bind with RBM3 pre-mRNA to promote circ0008399 formation[26]. In this study, we found that the expression of EIF4A3 was increased after KO of ARID1A in EJ and T24T cells (fig. 4A–4C). To further explore whether the EIF4A3 inhibitor is an alternative therapeutic strategy that could improve CDDP-based therapy effects in ARID1A-deficient BC, we selected EIF4A3-IN-2, a highly specific small molecule EIF4A3 inhibitor, to inhibit the function of EIF4A3. The results showed that the expression of circ0008399 was reduced in EJ and T24T cells treated with EIF4A3-IN-2 (fig. 4D). Moreover, we further confirmed that the EIF4A3 inhibitor reversed the reduction of cell apoptosis induced by ARID1A KO upon CDDP treatment (fig. 4E–4H). Collectively, these results suggested that inhibition of EIF4A3 could be a potential therapeutic strategy to enhance CDDP sensitivity in ARID1A-deficient BC cells.

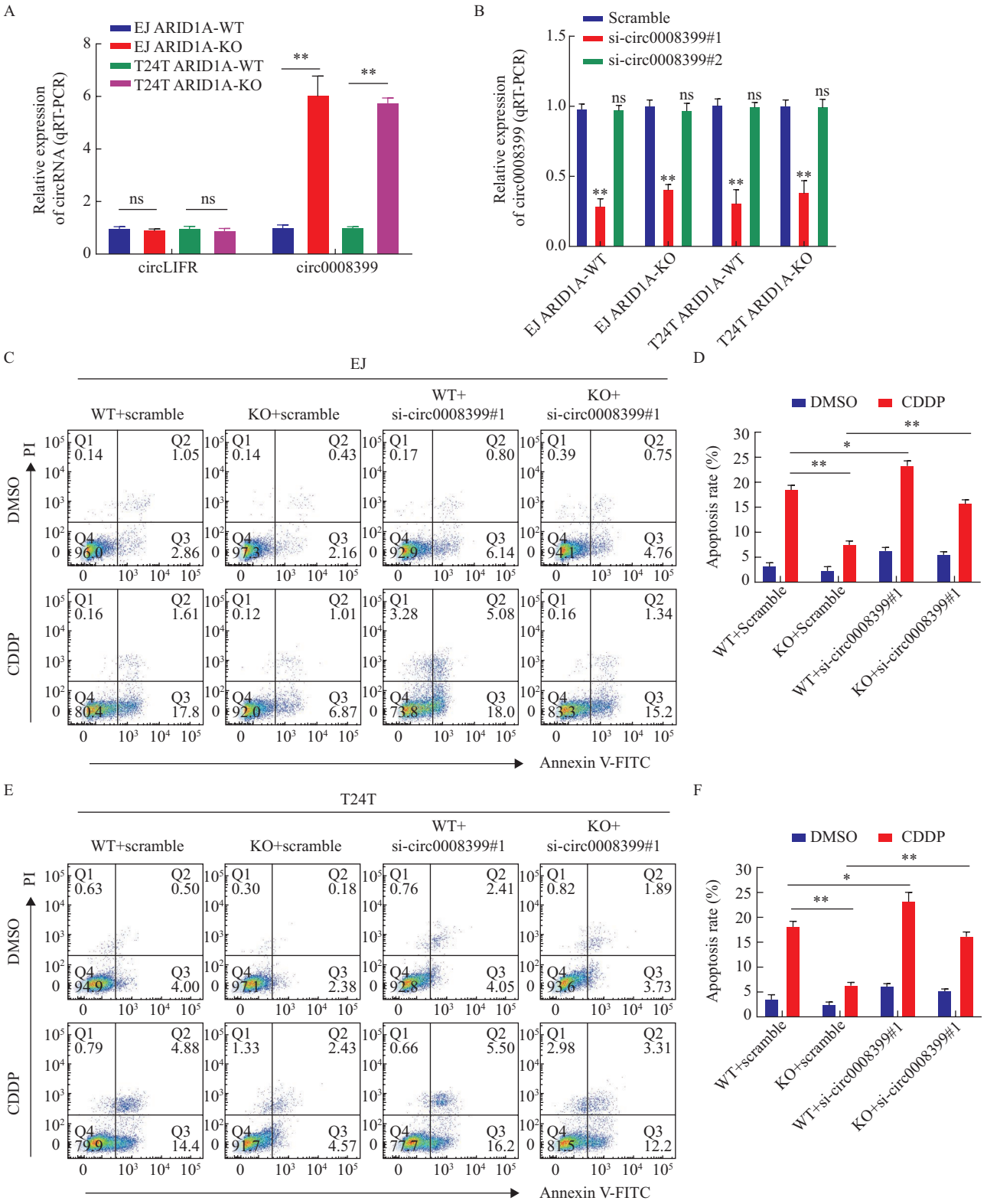

Fig. 3 Loss of ARID1A induces the expression of circ0008399

A: The expression levels of circ0008399 and circLIFR were detected by qRT-PCR in EJ and T24T cells of ARID1A-WT and ARID1A-KO. B: The expression levels of circ0008399 were detected by qRT-PCR in EJ and T24T cells transfected with si-circ0008399#1, si-circ0008399#2, or a corresponding scramble. C and D: Flow cytometry showed the apoptosis rate of ARID1A-WT and ARID1A-KO EJ cells transfected with scramble or si-circ0008399#1, after treatment of 5 μmol/L CDDP or PBS for 24 h. E and F: Flow cytometry showed the apoptosis rate of ARID1A-WT and ARID1A-KO T24T cells transfected with scramble or si-circ0008399#1, after treatment of 5 μmol/L CDDP or PBS for 24 h. Data were expressed as the mean ± SD (n=3) of the individual experiments. Statistical significance was assessed by student's t test (A), one-way ANOVA (B), and three-way ANOVA (D and F). $^{*}P$<0.05, $^{**}P$<0.01. ARID1A: AT-rich interaction domain 1A; BC: bladder cancer; CDDP: cisplatin; circ0008399: circular RNA 0008399; DMSO: dimethyl sulfoxide; KO: knockout; ns: not significant; PBS: phosphate buffered saline; qRT-PCR: quantitative real time polymerase chain reaction; SD: standard deviation; WT: wild-type

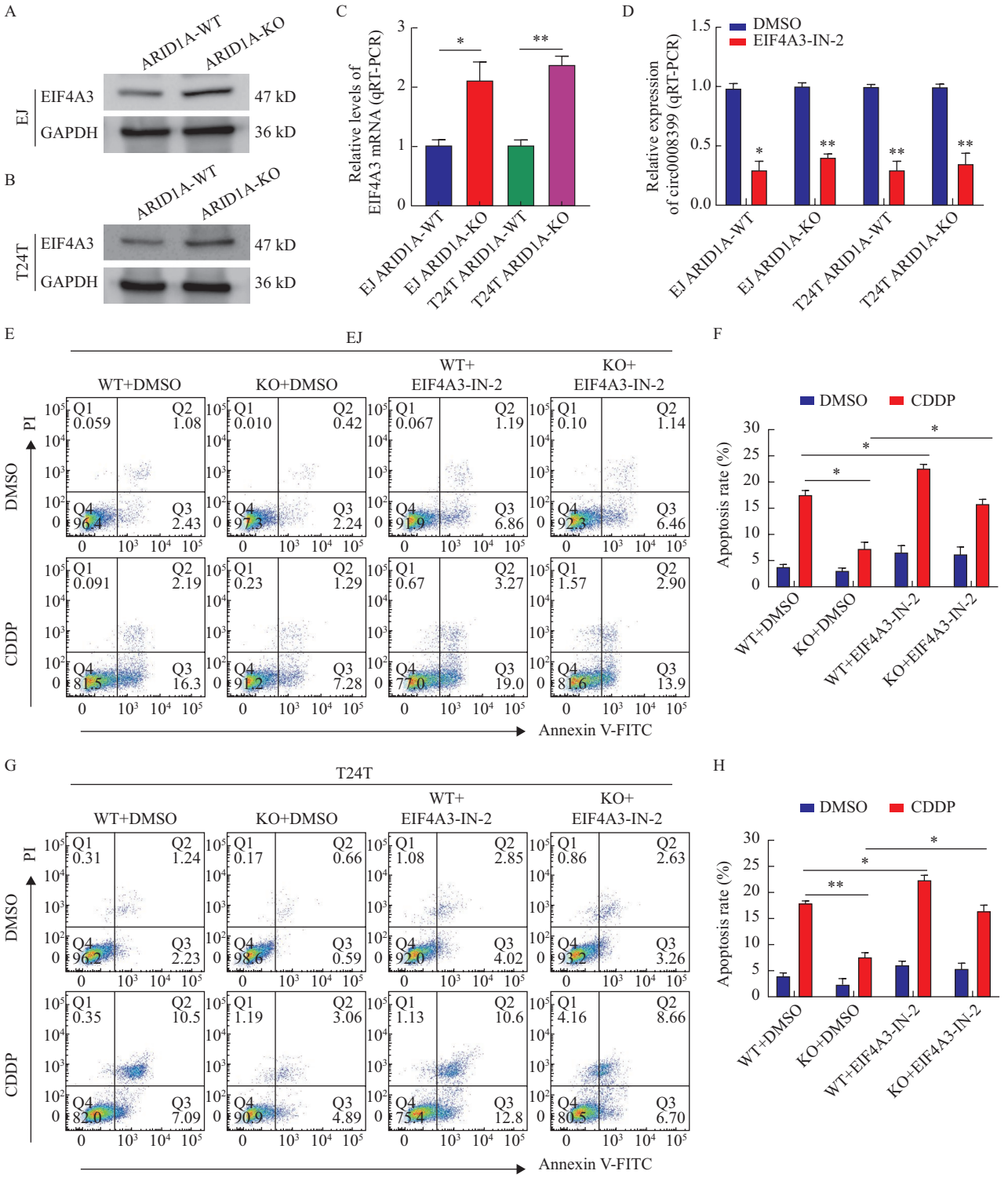

Fig. 4 EIF4A3-IN-2 promotes the chemosensitivity of ARID1A-deficient bladder tumor to CDDP

A and B: The protein expression levels of EIF4A3 were detected by Western blotting in (A) EJ and (B) T24T cells of ARID1A-WT and ARID1A-KO. Protein levels were normalized by GAPDH. C: The mRNA expression levels of EIF4A3 were detected by qRT-PCR in EJ and T24T cells of ARID1A-WT and ARID1A-KO. D: The expression levels of circ0008399 were detected by qRT-PCR in EJ and T24T cells of ARID1A-WT and ARID1A-KO, after treatment of 110 nmol/L EIF4A3-IN-2 for 36 h. E and F: Flow cytometry showed the apoptosis rate of ARID1A-WT and ARID1A-KO EJ cells administered with DMSO or EIF4A3-IN-2 (110 nmol/L), after treatment of 5 μmol/L CDDP or DMSO for 24 h. G and H: Flow cytometry showed the apoptosis rate of ARID1A-WT and ARID1A-KO T24T cells administered with DMSO or EIF4A3-IN-2 (110 nmol/L), after treatment of 5 μmol/L CDDP or DMSO for 24 h. The data were expressed as the mean ± SD (n=3) of the individual experiments. Statistical significance was assessed by a student's t test (C and D) and a three-way ANOVA (F and H). $^{*}P$<0.05, $^{**}P$<0.01. ARID1A: AT-rich interaction domain 1A; BC: bladder cancer; CDDP: cisplatin; circ0008399: circular RNA 0008399; DMSO: dimethyl sulfoxide; EIF4A3: eukaryotic initiation factor 4A3; EIF4A3-IN-2: eukaryotic initiation factor 4A3 inhibitor compound 2; GAPDH: glyceraldehyde-3-phosphate dehydrogenase; KO: knockout; qRT-PCR: quantitative real time polymerase chain reaction; SD: standard deviation; WT: wild-type

2.5 Loss of ARID1A Reduces HDAC1 Recruitment and Increases Histone H4 Acetylation to Enhance BRD4-driven EIF4A3 Transcriptional Activation

Next, we further explored the mechanism underlying loss of ARID1A-upregulated EIF4A3 expression. Previous reports have shown that ARID1A regulates histone H4 acetylation by interacting with histone deacetylase 1 (HDAC1) to inhibit BRD4-driven transcriptional activation in BC[31]. Consistently, loss of ARID1A in non-small cell lung cancer leads to decreased recruitment of HDAC1 and inhibition of histone H4 deacetylation which promotes BRD4-driven transcriptional activation[32]. In this study, we downloaded the processed ChIP-seq data of ARID1A, HDAC1, H4Ac, and BRD4 from the Cistrome data browser to carry out the bioinformatics analysis[33]. The results of bioinformatics analysis showed that ARID1A, HDAC1, H4Ac, and BRD4 could all bind to the promoter region of the EIF4A3 gene, and their ChIP-seq binding peaks were overlapping with each other, suggesting that their interaction in this space may affect the regulation of EIF4A3 gene expression (fig. 5A). Next, we performed ChIP assays using antibodies against HDAC1, pan-acetylated H4Ac, and BRD4 in BC cells. The results showed that KO of ARID1A decreased the relative amount of HDAC1 binding to the EIF4A3 promoter in EJ and T24T cells (fig. 5B and 5C; fig. S1A), and the relative acetylation level of histone H4 in the EIF4A3 promoter region was upregulated (fig. 5D and 5E, fig. S1B). Meanwhile, KO of ARID1A increased the relative level of BRD4 binding to the EIF4A3 promoter in EJ and T24T cells (fig. 5F and 5G; fig. S1C). Furthermore, we found that the expression levels of EIF4A3 and circ0008399 were suppressed by JQ1 to inhibit BRD4 function in ARID1A-KO EJ and T24T cells (fig. 5H–5J). Taken together, these results indicate that loss of ARID1A could downregulate HDAC1 binding to enhance H4Ac in the EIF4A3 promoter and promote BRD4-driven transcriptional activation of EIF4A3, which results in increased circ0008399 expression and mediates the resistance of BC cells to CDDP chemotherapy (fig. 6).

3 DISCUSSION

BC is the most common urinary malignancy worldwide[34], and CDDP-based chemotherapy is critical for the survival and prognosis of patients with MIBC or metastatic BC[35]. Clinically, resistance to cisplatin therapy is a major problem and contributes to poor patient outcomes[35]. With the development of sequencing technology and clinical popularization, more and more genetic alterations have been found to be related to chemotherapy sensitivity of tumors, which makes it possible for targeted combination therapy to eliminate chemotherapy resistance. Previous studies have shown that ARID1A deficiency was associated with chemotherapy sensitivity in a variety of tumors. Loss of ARID1A correlated with shorter progression-free survival of patients with ovarian clear cell carcinomas treated with platinum-based chemotherapy[36], and ARID1A gene silencing reduces the sensitivity of ES2 OCCC cells to cisplatin in ovarian clear cell carcinoma[18]. And loss of ARID1A increased the sensitivity of noradrenergic cells by promoting the transition of noradrenergic cells from an adrenergic to a mesenchymal cell state[37]. In this study, we found that KO of ARID1A promoted cisplatin resistance in BC. However, there is still a lack of research which can effectively improve the sensitivity of AR1D1A inactivating mutant BC to chemotherapy. Here, we demonstrated that inactivation of ARID1A promoted the expression of circ0008399 through epigenetic activation of EIF4A3, and circ0008399 was critical for the survival of ARID1A-deficient BC in the presence of CDDP, which was different from the mechanism by which ARID1A silencing caused CDDP resistance in ovarian cancer. It indicated that CDDP resistance in tumors was multi-mechanism and meant that the same drug may have multiple different resistance mechanisms in different tumors. Elucidating mechanisms of different types of drug resistance will provide more potential targets for solving drug resistance. Importantly, our results indicated that the small molecule inhibitor EIF4A3-IN-2 specifically increased the chemical sensitivity of ARID1A deficient tumors to CDDP. These findings provide novel evidence that combined targeted inhibition of EIF4A3 could significantly increase the response of ARID1A deficient BC to first-line CDDP chemotherapy.

The SWI/SNF complex contributes to epigenetic regulation by utilizing the energy of ATP hydrolysis to remodel chromatin and thus regulate the transcription of target genes[38]. The ARID1A truncation mutation is considered to be by far the most common alteration of the SWI/SNF complex in urothelial bladder cancer[39]. ARID1A mutations occur in approximately 20% of urothelial carcinomas, with loss of the product of this tumor suppressor gene[40, 41]. As a core component of the SWI/SNF chromatin remodeling complex, mutations in ARID1A affect many important biological processes such as transcriptional regulation[42]. For example, on the one hand, it has been reported that two key components of the SWI/SNF complex, BRG1 and BAF155, were no longer recruited to chromatin in ARID1A KO breast cancer cells. This resulted in a significant reduction in chromatin openness and binding ability of FOXA1 or other transcription factors to target chromatin regions, which downregulated the transcriptional activity of estrogen receptor genes[43]. On the other hand, recent studies have shown that loss of ARID1A could play a role in chromatin remodeling

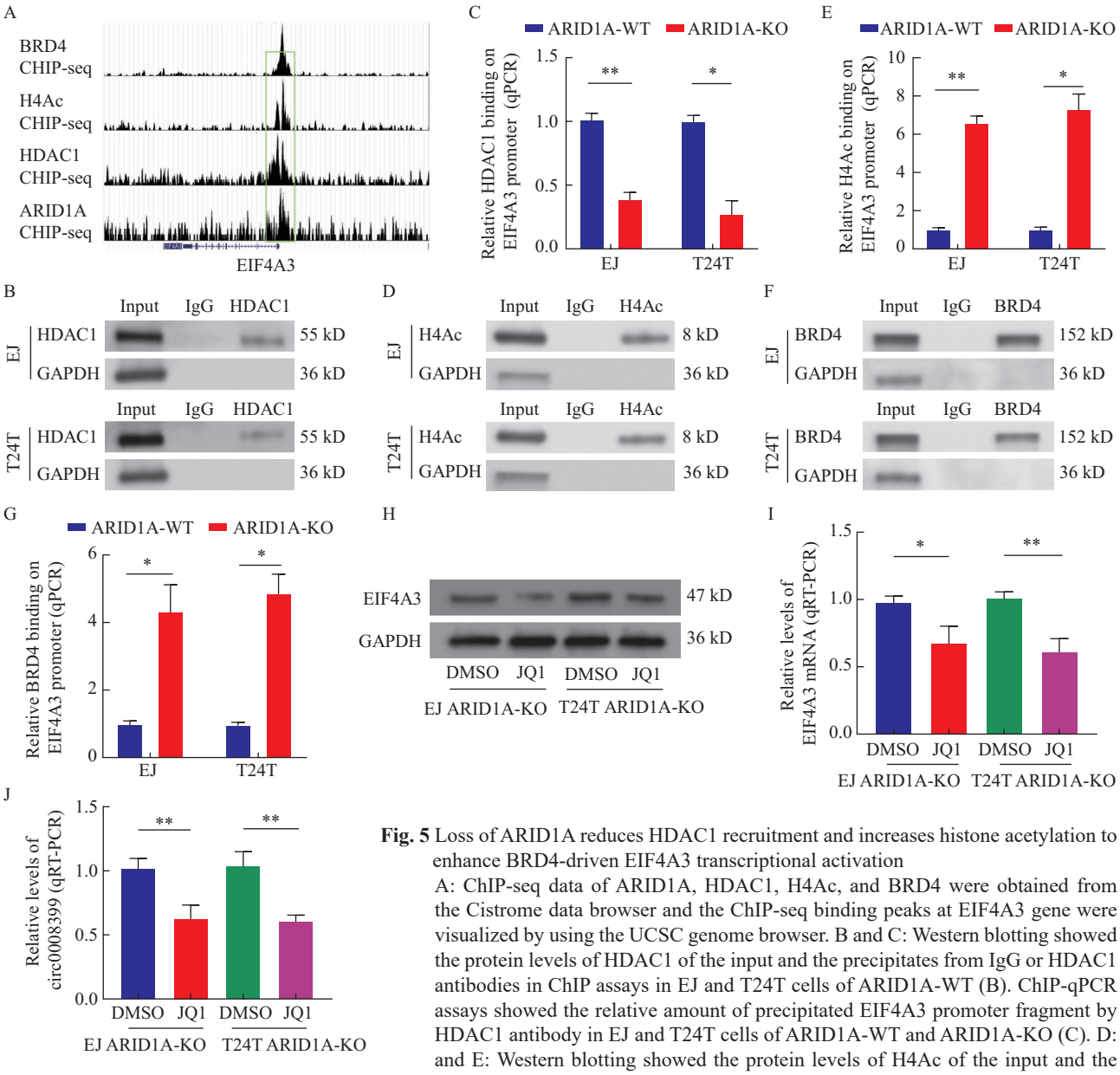

Fig. 5 Loss of ARID1A reduces HDAC1 recruitment and increases histone acetylation to enhance BRD4-driven EIF4A3 transcriptional activation

A: ChIP-seq data of ARID1A, HDAC1, H4Ac, and BRD4 were obtained from the Cistrome data browser and the ChIP-seq binding peaks at EIF4A3 gene were visualized by using the UCSC genome browser. B and C: Western blotting showed the protein levels of HDAC1 of the input and the precipitates from IgG or HDAC1 antibodies in ChIP assays in EJ and T24T cells of ARID1A-WT (B). ChIP-qPCR assays showed the relative amount of precipitated EIF4A3 promoter fragment by HDAC1 antibody in EJ and T24T cells of ARID1A-WT and ARID1A-KO (C). D: and E: Western blotting showed the protein levels of H4Ac of the input and the precipitates from IgG or H4Ac antibodies in ChIP assays in EJ and T24T cells of ARID1A-WT. E: ChIP-qPCR assays showed the relative amount of precipitated EIF4A3 promoter fragment by H4Ac antibody in EJ and T24T cells of ARID1A-WT and ARID1A-KO. F: Western blotting showed the protein levels of BRD4 of the input and the precipitates from IgG or BRD4 antibodies in ChIP assays in EJ and T24T cells of ARID1A-WT. G: ChIP-qPCR assays showed the relative amount of precipitated EIF4A3 promoter fragment by BRD4 antibody in EJ and T24T cells of ARID1A-WT and ARID1A-KO. H and I: The protein expression levels of EIF4A3 were detected by Western blotting in EJ ARID1A-KO and T24T ARID1A-KO cells treated with JQ1 or DMSO. Protein levels were normalized by GAPDH (H). The mRNA expression levels of EIF4A3 were detected by qRT-PCR in EJ ARID1A-KO and T24T ARID1A-KO cells treated with JQ1 or DMSO (I). J: The expression levels of circ0008399 were detected by qRT-PCR in EJ ARID1A-KO and T24T ARID1A-KO cells treated with JQ1 or DMSO. The data are expressed as the mean ± SD (n=3) of the individual experiments. Statistical significance was determined with a student's t test. $^{*}P$<0.05 (C, E, G, I, and J), $^{**}P$<0.01. ARID1A: AT-rich interaction domain 1A; BRD4: bromodomain containing 4; ChIP: chromatin immunoprecipitation; ChIP-qPCR: chromatin immunoprecipitation-quantitative real time polymerase chain reaction; circ0008399: circular RNA 0008399; DMSO: dimethyl sulfoxide; EIF4A3: eukaryotic initiation factor 4A3; GAPDH: glyceraldehyde-3-phosphate dehydrogenase; H4Ac: histone H4 acetylation; HDAC1: histone deacetylase 1; JQ1: BET bromodomain inhibitor (+)-JQ-1; KO: nockout; SD: standard deviation; WT: wild-type

through ARID1B-dependent functional compensation, which promotes SP1 binding to chromatin sites to activate the human endogenous retrovirus-H (HERVH) transcription[44]. Meanwhile, recent discoveries also suggest that ARID1A inactivation could promote the development of non-small cell lung cancer by reducing HDAC1 recruited to chromatin and inhibiting histone H4 deacetylation in the corresponding regions, thereby promoting the recruitment of BRD4, increasing chromatin accessibility, and enhancing the binding of HIF1α to the promoter regions of glycolytic related genes to activate the expression of related target

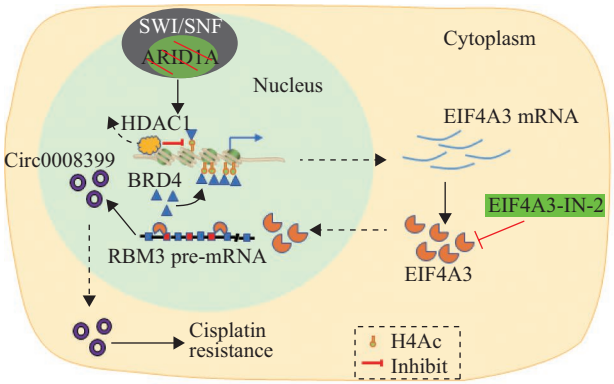

Fig. 6 Model depicting the proposed effects of ARID1A-deficiency on the sensitivity of bladder cancer to CDDP BRD4: bromodomain containing 4; circ0008399: circular RNA 0008399; EIF4A3: eukaryotic initiation factor 4A3; H4Ac: histone H4 acetylation; HDAC1: histone deacetylase 1; Pre-mRNA: precursor messenger RNA; RBM3: RNA binding motif protein 3; SWI/SNF: switching/sucrose non-fermentable

genes[32]. In this study, we found that loss of ARID1A in BC could increase histone H4 acetylation by affecting HDAC1 function, thereby promoting BRD4-driven transcriptional activation of the EIF4A3 gene. Our study further demonstrates that ARID1A plays a key role in epigenetic regulation in BC.

EIF4A3 is a core component of the splicing-dependent multiprotein exon junction complex (EJC). As one of the RNA binding proteins (RBPs), EIF4A3 regulates the generation of a series of circRNAs[45, 46]. An increasing number of studies have shown that EIF4A3 affects the chemotherapy sensitivity of various tumors by promoting the production of circRNAs. For example, EIF4A3 promoted the expression of circRAB3IP and reduced the sensitivity of prostate cancer to enzalutamide[47]. EIF4A3-induced circular RNA ASAP1 (circASAP1) promotes temozolomide resistance of glioblastoma via NRAS/MEK1/ERK1/2 signaling[48], and EIF4A3-induced circular RNA PRKAR1B (cirPRKAR1B) suppresses the sensitivity of osteosarcoma cells to CDDP[49]. Our recent study showed that EIF4A3 promoted the production of circ0008399 in BC, thus enhancing the resistance of BC cells to CDDP[26]. Here, we further found that inactivation of ARID1A could enhance the expression of EIF4A3 to promote the expression of circ0008399 and mediate the resistance of BC to CDDP, which provides a new insight for further understanding the role of EIF4A3-induced circRNAs expression in the regulation of chemotherapy sensitivity in cancer cells.

In conclusion, we demonstrate that ARID1A inactivated BC cells are less sensitive to CDDP, and inhibition of EIF4A3 activity could downregulate circ0008399 expression, thereby enhancing the sensitivity of ARID1A-deficient BC cells to CDDP. Therefore, our results suggest an effective targeted combination therapy to improve chemotherapy sensitivity in ARID1A deficient bladder cancer patients.

Conflict of Interest Statement

The authors declare that they have no conflicts of interest.

REFERENCES

1 Sung H, Ferlay J, Siegel RL, *et al*. Global Cancer Statistics 2020: GLOBOCAN Estimates of Incidence and Mortality Worldwide for 36 Cancers in 185 Countries. CA Cancer J Clin, 2021,71(3):209-249
2 Tavora F, Epstein JI. Bladder cancer, pathological classification and staging. BJU Int, 2008,102(9 Pt B):1216-1220
3 Millan-Rodriguez F, Chechile-Toniolo G, Salvador-Bayarri J, *et al*. Multivariate analysis of the prognostic factors of primary superficial bladder cancer. J Urol, 2000,163(1):73-78
4 Kamoun A, de Reynies A, Allory Y, *et al*. A Consensus Molecular Classification of Muscle-invasive Bladder Cancer. Eur Urol, 2020,77(4):420-433
5 Kamat AM, Hegarty PK, Gee JR, *et al*. ICUD-EAU International Consultation on Bladder Cancer 2012: Screening, diagnosis, and molecular markers. Eur Urol, 2013,63(1):4-15
6 Witjes JA, Bruins HM, Cathomas R, *et al*. European Association of Urology Guidelines on Muscle-invasive and Metastatic Bladder Cancer: Summary of the 2020 Guidelines. Eur Urol, 2021,79(1):82-104
7 Galluzzi L, Senovilla L, Vitale I, *et al*. Molecular mechanisms of cisplatin resistance. Oncogene, 2012, 31(15):1869-83
8 Valle JW, Lamarca A, Goyal L, *et al*. New Horizons for Precision Medicine in Biliary Tract Cancers. Cancer Discov, 2017,7(9):943-962
9 Lu C, Allis CD. SWI/SNF complex in cancer. Nat Genet, 2017,49(2):178-179
10 Wu JN, Roberts CW. ARID1A mutations in cancer: another epigenetic tumor suppressor? Cancer Discov, 2013,3(1):35-43
11 Mathur R, Alver BH, San Roman AK, *et al*. ARID1A loss impairs enhancer-mediated gene regulation and drives colon cancer in mice. Nat Genet, 2017,49(2):296-302
12 Wu RC, Wang TL, Shih Ie M. The emerging roles of ARID1A in tumor suppression. Cancer Biol Ther, 2014,15(6):655-664
13 Megino-Luque C, Siso P, Mota-Martorell N, *et al*. ARID1A-deficient cells require HDAC6 for progression of endometrial carcinoma. Mol Oncol, 2022,16(11):2235-2259
14 Elkhadragy L, Dasteh Goli K, Totura WM, *et al*. Effect of CRISPR Knockout of AXIN1 or ARID1A on Proliferation and Migration of Porcine Hepatocellular Carcinoma. Front Oncol, 2022,12:904031
15 Shang XY, Shi Y, He DD, *et al*. ARID1A deficiency weakens BRG1-RAD21 interaction that jeopardizes chromatin compactness and drives liver cancer cell metastasis. Cell Death Dis, 2021,12(11):990
16 Liu X, Dai SK, Liu PP, *et al*. Arid1a regulates neural stem/progenitor cell proliferation and differentiation during cortical development. Cell Prolif, 2021,54(11):e13124
17 Zhang FK, Ni QZ, Wang K, *et al*. Targeting USP9X-

AMPK Axis in ARID1A-Deficient Hepatocellular Carcinoma. Cell Mol Gastroenterol Hepatol, 2022,14 (1):101-127
18 Lyu C, Zhang Y, Zhou X, *et al*. ARID1A gene silencing reduces the sensitivity of ovarian clear cell carcinoma to cisplatin. Exp Ther Med, 2016,12(6):4067-4071
19 Nigro JM, Cho KR, Fearon ER, *et al*. Scrambled exons. Cell, 1991,64(3):607-613
20 Goodall GJ, Wickramasinghe VO. RNA in cancer. Nat Rev Cancer, 2021,21(1):22-36
21 Li Y, Zheng F, Xiao X, *et al*. CircHIPK3 sponges miR-558 to suppress heparanase expression in bladder cancer cells. EMBO Rep, 2017,18(9):1646-1659
22 Xie F, Li Y, Wang M, *et al*. Circular RNA BCRC-3 suppresses bladder cancer proliferation through miR-182-5p/p27 axis. Mol Cancer, 2018,17(1):144
23 Xie F, Xiao X, Tao D, *et al*. circNR3C1 Suppresses Bladder Cancer Progression through Acting as an Endogenous Blocker of BRD4/C-myc Complex. Mol Ther Nucleic Acids, 2020,22:510-519
24 Liu F, Zhang H, Xie F, *et al*. Correction: Hsa_ circ_0001361 promotes bladder cancer invasion and metastasis through miR-491-5p/MMP9 axis. Oncogene, 2022,41(35):4183
25 Zhang H, Xiao X, Wei W, *et al*. CircLIFR synergizes with MSH2 to attenuate chemoresistance via MutSalpha/ATM-p73 axis in bladder cancer. Mol Cancer, 2021,20(1):70
26 Wei W, Sun J, Zhang H, *et al*. Circ0008399 Interaction with WTAP Promotes Assembly and Activity of the m(6)A Methyltransferase Complex and Promotes Cisplatin Resistance in Bladder Cancer. Cancer Res, 2021,81(24):6142-6156
27 Iwatani-Yoshihara M, Ito M, Ishibashi Y, *et al*. Discovery and Characterization of a Eukaryotic Initiation Factor 4A-3-Selective Inhibitor That Suppresses Nonsense-Mediated mRNA Decay. ACS Chem Biol, 2017,12(7):1760-1768
28 Xu Y, Zhang S, Liao X, *et al*. Circular RNA circIKBKB promotes breast cancer bone metastasis through sustaining NF-kappaB/bone remodeling factors signaling. Mol Cancer, 2021,20(1):98
29 Filippakopoulos P, Qi J, Picaud S, *et al*. Selective inhibition of BET bromodomains. Nature, 2010,468 (7327):1067-1073
30 Tao J, Lu Q, Wu D, *et al*. microRNA-21 modulates cell proliferation and sensitivity to doxorubicin in bladder cancer cells. Oncol Rep, 2011,25(6):1721-1729
31 Nagarajan S, Rao SV, Sutton J, *et al*. ARID1A influences HDAC1/BRD4 activity, intrinsic proliferative capacity and breast cancer treatment response. Nat Genet, 2020,52(2):187-197
32 Liu X, Li Z, Wang Z, *et al*. Chromatin Remodeling Induced by ARID1A Loss in Lung Cancer Promotes Glycolysis and Confers JQ1 Vulnerability. Cancer Res, 2022,82(5):791-804
33 Mei S, Qin Q, Wu Q, *et al*. Cistrome Data Browser: a data portal for ChIP-Seq and chromatin accessibility data in human and mouse. Nucleic Acids Res, 2017,45(D1):D658-D662
34 Iyer G, Rosenberg JE. Novel therapies in urothelial carcinoma: a biomarker-driven approach. Ann Oncol, 2018,29(12):2302-2312
35 von der Maase H, Hansen SW, Roberts JT, *et al*. Gemcitabine and cisplatin versus methotrexate, vinblastine, doxorubicin, and cisplatin in advanced or metastatic bladder cancer: results of a large, randomized, multinational, multicenter, phase III study. J Clin Oncol, 2000,18(17):3068-3077
36 Katagiri A, Nakayama K, Rahman MT, *et al*. Loss of ARID1A expression is related to shorter progression-free survival and chemoresistance in ovarian clear cell carcinoma. Mod Pathol, 2012,25(2):282-288
37 Shi H, Tao T, Abraham BJ, *et al*. ARID1A loss in neuroblastoma promotes the adrenergic-to-mesenchymal transition by regulating enhancer-mediated gene expression. Sci Adv, 2020,6(29):eaaz3440
38 Wang X, Sansam CG, Thom CS, *et al*. Oncogenesis caused by loss of the SNF5 tumor suppressor is dependent on activity of BRG1, the ATPase of the SWI/SNF chromatin remodeling complex. Cancer Res, 2009,69(20):8094-8101
39 Garczyk S, Schneider U, Lurje I, *et al*. ARID1A-deficiency in urothelial bladder cancer: No predictive biomarker for EZH2-inhibitor treatment response? PLoS One, 2018,13(8):e0202965
40 Li J, Lu S, Lombardo K, *et al*. ARID1A alteration in aggressive urothelial carcinoma and variants of urothelial carcinoma. Hum Pathol, 2016,55:17-23
41 Wang F, Dong X, Yang F, *et al*. Comparative Analysis of Differentially Mutated Genes in Non-Muscle and Muscle-Invasive Bladder Cancer in the Chinese Population by Whole Exome Sequencing. Front Genet, 2022,13:831146
42 Conde M, Frew IJ. Therapeutic significance of ARID1A mutation in bladder cancer. Neoplasia (New York, NY), 2022,31:100814
43 Xu G, Chhangawala S, Cocco E, *et al*. ARID1A determines luminal identity and therapeutic response in estrogen-receptor-positive breast cancer. Nat Genet, 2020,52(2):198-207
44 Yu C, Lei X, Chen F, *et al*. ARID1A loss derepresses a group of human endogenous retrovirus-H loci to modulate BRD4-dependent transcription. Nat Commun, 2022,13(1):3501
45 Conn SJ, Pillman KA, Toubia J, *et al*. The RNA binding protein quaking regulates formation of circRNAs. Cell, 2015,160(6):1125-34
46 Chan CC, Dostie J, Diem MD, *et al*. eIF4A3 is a novel component of the exon junction complex. RNA, 2004,10(2):200-209
47 Chen D, Wang Y, Yang F, *et al*. The circRAB3IP Mediated by eIF4A3 and LEF1 Contributes to Enzalutamide Resistance in Prostate Cancer by Targeting miR-133a-3p/miR-133b/SGK1 Pathway. Front Oncol, 2021,11:752573
48 Wei Y, Lu C, Zhou P, *et al*. EIF4A3-induced circular RNAASAP1 promotes tumorigenesis and temozolomide resistance of glioblastoma via NRAS/MEK1/ERK1-2 signaling. Neuro Oncol, 2021,23(4):611-624
49 Feng ZH, Zheng L, Yao T, *et al*. EIF4A3-induced circular RNA PRKAR1B promotes osteosarcoma progression by miR-361-3p-mediated induction of FZD4 expression. Cell Death Dis, 2021,12(11):1025

(Received Jan. 2, 2023; accepted Feb. 20, 2023)